Two approaches for orientation field segmentation based on directional morphology

LUIS A. MORALES-HERNÁNDEZ[1], FEDERICO MANRÍQUEZ-GUERRERO[2]
and IVÁN R. TEROL-VILLALOBOS[2]

[1] *Doctorado en Ingeniería, Universidad Autónoma de Querétaro, Mexico*
`luis_morah@yahoo.com`

[2] *Centro de Investigación y Desarrollo Tecnológico en Electroquímica S. C. (CIDETEQ),
Parque Tecnológico Querétaro, Mexico*
`{fmanriquez,iterol}@cideteq.mx`

Abstract   In the present paper, morphological approaches for segmenting orientation fields are proposed. First, it is investigated the use of directional granulometries and a quadtree structure to extract the main directional structures of the image. Then, it is proposed a method based on the concept of the line-segment and orientation functions. The line-segment function is computed from the supremum of directional erosions. This function contains the sizes of the longest lines that can be included in the structure. On the other hand, the orientation function contains their angles. Combining both functions permits the construction of a weighted partition using the watershed transformation. Finally, the elements of the partition are merged using a region adjacency graph (RAG) structure.

Keywords: directional morphology, directional granulometry, orientation fields, line-segment function, orientation function, watershed transform.

1.   Introduction

Even if anisotropic structures are frequently found in many classes of images (materials, biometry images, biology, ...), few works dealing with directional analysis in morphological image processing have been carried out. From an algorithmic point of view one has [14, 15] among others, while in application some references are [5, 16]. It is in the domain of fingerprint recognition, which is today the most widely used biometric features for personal identification, where the study of directional structures based on orientation-field detection is an active subject of research [2, 7, 9]. In fact, fingerprints can be considered as a structure composed by a set of line segments (see Figure 1(a)). However, the orientation-field detection also plays a fundamental role in other domains [1, 6]. For example, in materials, the pearlite phase

displays a morphology in the form of parallel lines (see Figure 1(b)) and when forming another grain, these can change of direction. In this case, field extraction from an image is a useful technique for the characterization of the pearlitic phase.

Given the interest in orientation pattern models for characterizing structures, this paper investigates the use of the mathematical morphology for modelling orientation fields. As for the human vision, computer image processing of oriented image structures often requires a bank of directional filters or template masks, each of them sensitive to a specific range of orientations. Then, one investigates first the use of directional granulometries, computed by morphological openings, using directional structuring elements. This approach allows one to determine the main directions of the structures by identifying the minima of the granulometric distribution function. In order to define a local approach, a quadtree structure is used to decompose the image with different resolution according to the levels of the tree.

After illustrating some drawbacks of using a bank of morphological filters (openings) and a quadtree structure to characterize orientation fields, one introduces an approach based on directional erosions. This method considers a local approach using the concept of line-segment function combined with the watershed transformation. In our case, the line-segment function is computed from the supremum of directional erosions. This function contains the information of the longest line segments that can be placed inside the structure. In order to know their orientation, a second image is defined by observing the construction of the line-segment function and its evolution. This second image is computed by detecting the orientation of the supremum of directional erosions. These local descriptors, for the element size and the orientation, enable the identification of the orientation fields based on the watershed transformation.

This paper is organized as follows. In Section 2, the concepts of morphological filter and directional morphology are presented. In Sections 3 and 4, a study for segmenting orientation fields based on the directional granulometry is carried out. Next, in Section 5 the notions of line-segment and orientation functions, derived from the supremum of directional erosions, are introduced. Finally, in Section 6 an approach of working with directional morphology, the watershed transform and a region adjacency graph (RAG) for segmenting orientation fields is proposed.

2.   Some basic concepts of morphological filtering

In mathematical morphology one calls morphological filter all increasing and idempotent transformation [4, 12]. The basic morphological filters are the morphological opening $\gamma_{\mu B}$ and the morphological closing $\varphi_{\mu B}$ given a structuring element B (for example a square of 3×3 pixels) and an homothetic parameter μ. Let $\check{B}$ is the transposed set of B ($\check{B} = \{-x :$

$x \in B\}$), the morphological opening and closing are given by: $\gamma_{\mu B}(f) = \delta_{\mu \check{B}}(\varepsilon_{\mu B}(f))$ and $\varphi_{\mu B}(f) = \varepsilon_{\mu \check{B}}(\delta_{\mu B}(f))$, where the morphological erosion $\varepsilon_{\mu B}$ and dilation $\delta_{\mu B}$ are expressed by $\varepsilon_{\mu B}(f)(x) = \wedge\{f(y) : y \in \mu \check{B}_x\}$ and $\delta_{\mu B}(f)(x) = \vee\{f(y) : y \in \mu \check{B}_x\}$, and where $\wedge$ is the infimum and $\vee$ is the supremum.

Morphological directional transformations are characterized by two parameters. Their structuring elements are line segments L having a length (size μ) and a slope (angle α). For $\alpha \in [0, 90]$, the line segment $L(\alpha, \mu)$ is formed of the set of points $\{(x_i, y_i)\}$ computed using the following expressions:

if $0 \leq \alpha \leq 45$ then, $y_i = x_i tan(\alpha)$ for $x_i = 0, 1, \cdots, (\mu/2)cos(\alpha)$,

if $90 \geq \alpha > 45$ then, $x_i = y_i cot(\alpha)$ for $y_i = 0, 1, \cdots, (\mu/2)cos(\alpha)$,

and of the set of points $\{(-x_i, -y_i)\}$.

In this way, the structuring element is a symmetric, i.e., $L(\alpha, \mu) = \hat{L}(\alpha, \mu)$. Similar expressions can be used for $\alpha \in (90, 180]$.

For the sake of simplicity, from now on, we will denote the morphological opening $\gamma_{L(\alpha, \mu)}$ and closing $\varphi_{L(\alpha, \mu)}$, respectively, $\gamma_{\alpha, \mu}$ and $\varphi_{\alpha, \mu}$.
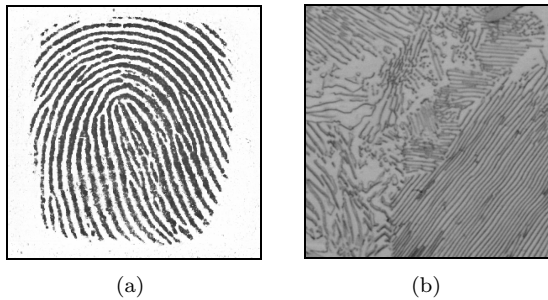

(a)   (b)

Figure 1. (a) Fingerprint image. (b) Pearlitic phase image.

3. Directional granulometry

Granulometry was formalized by Matheron for binary images and extended to complete lattices by Serra [12]. Granulometry is defined as follows:

Definition 1 (Granulometry). A family of openings $\{\gamma_{\mu_i}\}$ (or respectively of closings $\{\varphi_{\mu_i}\}$), where $i \in \{1, 2, \ldots n\}$, is a granulometry (respectively antigranulometry) if for all $i, j \in \{1, 2, \ldots n\}$ and for all function f,

$$\mu_i \leq \mu_j \Rightarrow \gamma_{\mu_i}(f) \geq \gamma_{\mu_j}(f) \qquad (\text{resp. } \varphi_{\mu_i}(f) \leq \varphi_{\mu_j}(f)).$$
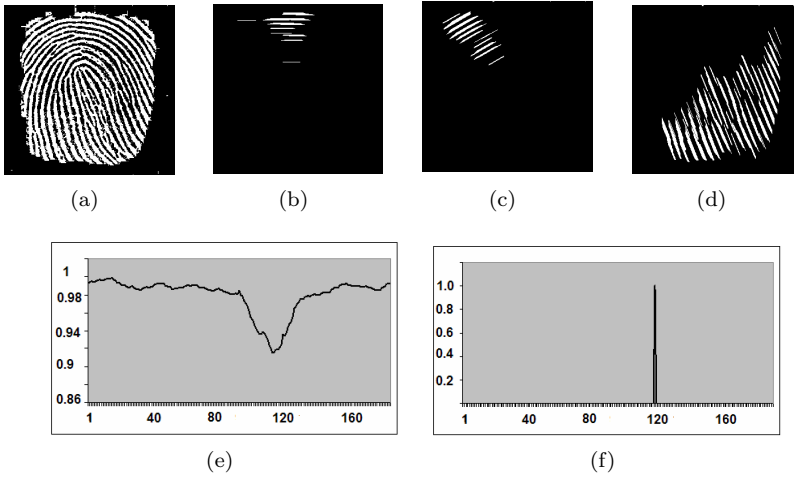
$\square$

Figure 2. (a) Binary image. (b–d) Directional opening of size 80 and angles 0, 55, 112, respectively. (e) Granulometric curve computed from image (a). (f) Minima detection.

The ordering relationship implies that greater the parameter, more severe the opening (closing). The granulometric analysis of a binary or gray-level image, consists in associating with each μ_i value a measure of the image $\gamma_{\mu_i}(f)$. Two functions are associated to these transformations: the granulometric density function g and its distribution function G given respectively by:

$$g(\alpha,\lambda)(f) = (Mes(\gamma_{\alpha,\lambda+1})(f) - Mes(\gamma_{\alpha,\lambda})(f))/Mes(f),$$

$$G(\alpha,\lambda)(f) = (Mes(f) - Mes(\gamma_{\alpha,\lambda})(f))/Mes(f),$$

where *Mes* represents the volume for gray-level images and the area for binary images. To illustrate the use of the granulometry for detecting anisotropies inside a structure, the binary image of Figure 2(a) was computed from the gray-level image of Figure 1(a). Figures 2(b), 2(c) and 2(d), illustrate the output images computed from the image of Figure 2(a), using a directional opening of size $\mu = 80$ and angles 0, 55 and 112 degrees, respectively. Observe that this microstructure contains a main direction at approximately 112 degrees. To detect automatically the main direction in a structure one computes a granulometry as described below.
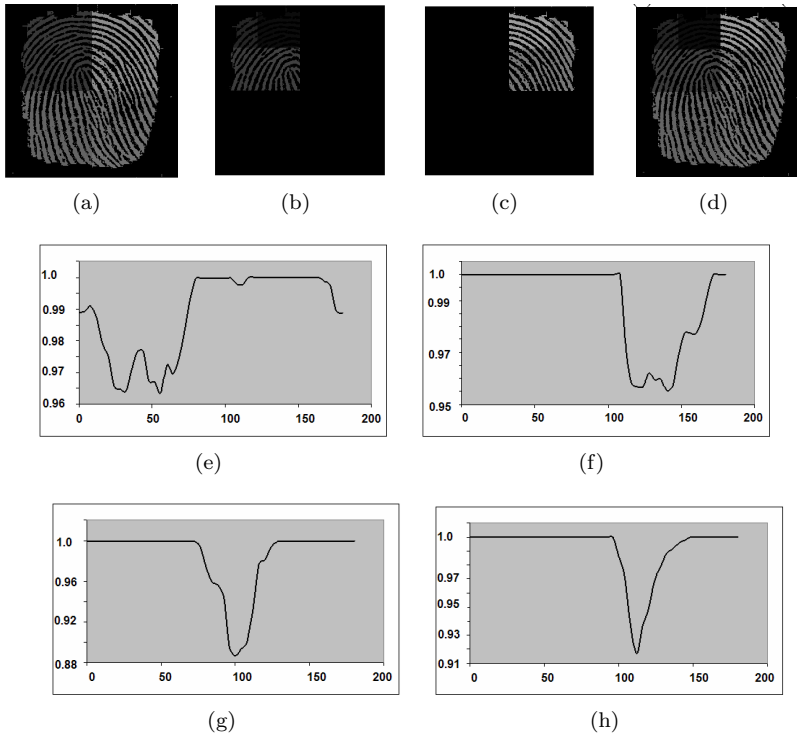
Figure 3. (a) First hierarchy of the quatree. (b, c) Second hierarchy of the quadtree. (d) Final segmentation. (e–h) Granulometric curves of the first hierarchy.

4.   Directional granulometry and quadtree structure

By computing the density function $g(\alpha, \lambda)$ one obtains the portion of the structure, for a given direction α, of size λ, whereas the distribution function $G(\alpha, \lambda)$ gives the fraction of the structures greater than or equal to the length λ in the direction α. This latter function is more interesting since it permits the selection of the main structures in a given direction. Thus, instead of fixing the parameter α, the parameter λ was fixed. Figure 2(e), illustrates the distribution function of the image of Figure 2(a), for $\lambda = 80$ and $0 < \alpha < 180$. This expression permits one to know the percentage of the structure removed by the opening.

For some angles the directional opening removes all of the structure, and $G(\alpha, \lambda)(f) \approx 1$, whereas in the direction of the longest structures $G(\alpha, \lambda)(f) < 1$. The global minimum of this function permits us to determine the direction of the main structures. The minimum in Figure 2(f), was computed from the function of Figure 2(e), using morphological trans-

formations in one-dimensional case. To carry out the minimum detection, the distribution function was scaled into the interval $[0, 255]$ in integer numbers and then, the traditional morphological tools for detecting minima in mathematical morphology were applied. In fact, the minima of the function will enable us to have a criterion to go from a global approach to a local one by means of the quadtree structure.

In the quadtree approach, the coding by regions is made by an homogeneity criterion (or criteria) that enables us to discriminate whether a square region can be considered a connected component. One starts with a square of 2^n pixels that is subdivided in four square zones. Each square zone is analyzed as a part of the original image using one or several homogeneity criteria (for example, variance, max-min values). If the homogeneity criterion (or criteria) is verified, a function value is given at all points of the square region (for example, the average of the intensity values in the square). For any square region that does not satisfy the homogeneity criterion, a similar procedure is performed in a recursive way by further dividing the square region by four.

For orientation fields, it is clear that an homogeneity criterion is given by a directional one and in our case, the minima of the distribution function are used as the criterion. If the distribution function in a square region presents only a principal minimum, then the region is considered homogeneous. In this case, the pixel values of the region are replaced by the angle of the minimum where the minimum was found. Otherwise, if the distribution function of a square region has several representative minima, then the region is devided again by four.

Figure 3(a) illustrates the approach to determine the orientation field in the image. After dividing the image by four (see Figure 3(a), the four distribution functions were computed as illustrated in Figures 3(e), 3(f), 3(g) and 3(h). In particular observe that the distribution functions of Figures 3(g) and 3(h), corresponding to the bottom right and left squares each contains only one principal minimum, while the other two squares, Figure 3(e) and Figure 3(f), contain several representative minima. Thus, these two squares were subdivided by four and their distribution functions were computed to know their directional homogeneity. Figure 3(c) illustrates the top square regions divided by four squares regions. Finally, Figure 3(d) illustrates the final hierarchy.

5. Size and orientation codification based on directional erosions

The approach described above for segmenting orientation fields has some main drawbacks. The first one is due to the fact that some regions must be processed several times (according to the hierarchy of the quadtree). A second problem is that the final segmentation will be composed by square
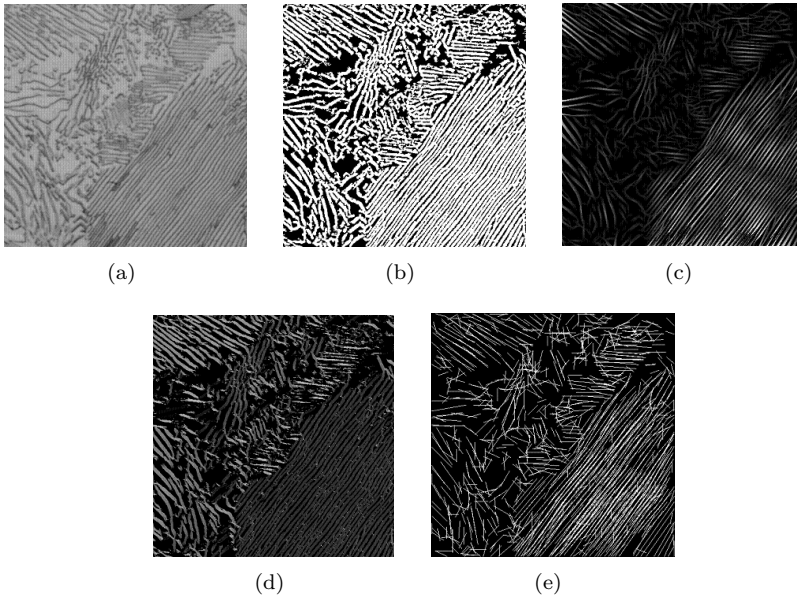
Figure 4. (a) Original image. (b) Binary image. (c, d) Line-segment and orientation functions. (e) Straight lines at the regional maxima of the line-segment function.

regions (or the union of square regions) which is not a real representation of image structures.

In this section and in the following ones we will look for another approach where the connectivity notion plays a fundamental role for segmenting the orientation fields. In fact, it is well-known that the notion of connectivity is linked to the intuitive idea of segmentation task, where the objective is to split the connected components in a set of elementary shapes that will be processed separately. Then, the problem lies in determining what a connected component is for an image such as those illustrated in Figure 1(a) and in Figure 1(b). Given that, we will look for another approach where the information of scales and directions of the structures of the image are easily accessible. Two functions that codify the size and the orientation are introduced below.

The idea for codifying size structure come from the notion of the distance function $D_X(x)$ that is a transformation that associates with each pixel x of a set X its distance from the background. The distance function can be computed by successive erosions of the set X. Let us now build a new function derived from the notion of distance function. The goal of building this function consists in codifying the size information in such a way that local directional information can be accessed from each point of the function.

This codification of the size information will be used to build a local

approach for detecting orientation fields on an image. This function, which we call line-segment function Dm, is computed by using the supremum of directional erosions. To stock the size information for all λ values, a gray-level image Dm is used. Thus, one begins with a small structuring element by taking into account all orientations to compute the set $\sup_{\alpha \in [0,180]} \{\varepsilon_{L(\lambda,\alpha)}(X)\}$. Then one increases $Dm(x)$ by one at all points x belonging to the set $\sup_{\alpha \in [0,180]} \{\varepsilon_{L(\lambda,\alpha)}(X)\}$, and one continues the procedure by increasing the size of the structuring element until the structure is completely removed. This means that the procedure continues until one has a $\lambda_{\max}$ value such that $\sup_{\alpha \in [0,180]} \{\varepsilon_{L(\lambda_{\max},\alpha)}(X)\} = \emptyset$. The maxima of the function Dm are the loci of longest structuring elements. Thus, one knows the position of the largest structuring elements that can be included completely in the structure.

However, the angles of these structuring elements (line segments) are not accessible from the image Dm. Therefore, one stocks the directions of the line segments in a second image Om, called orientation function, when the line-segment function is computed.

A real example (pearlitic phase) is shown in Figure 4(b), which is the binary image of that in Figure 4(a). The image of Figure 4(c) illustrates the line-segment function Dm whereas the image of Figure 4(d) shows the orientation Om function, computed from the binary image of Figure 4(b). Now, these functions can be now used for computing the line segments that characterize the structure. To illustrate the information contained in these images, the maxima of Dm were computed for obtaining the loci of the maximal structuring elements. Next, a line segment was placed at each maximum point x, with an angle given by $Om(x)$. The longest line segments in the image are illustrated in Figure 4(e). The line-segment function and its associated orientation image containing the angles, serve to suggest a method for segmenting images of orientation fields.

6. Image segmentation using directional morphology and the watershed transformation

Image segmentation is one of the most interesting problems in image processing and analysis. The main goal in image segmentation consists in extracting the regions of greatest interest in the image [3, 8]. A segmentation method must allow the introduction of specific criteria to obtain the desired regions (e.g., gray level, contrast, size, shape, texture, etc). In mathematical morphology, the watershed-plus-marker approach is the traditional image segmentation method [8]. This method has proved to be an efficient tool in many image-segmentation problems. Here, the watershed will be applied directly for obtaining a fine partition, and then a systematic merging process will be applied to obtain the final segmentation.

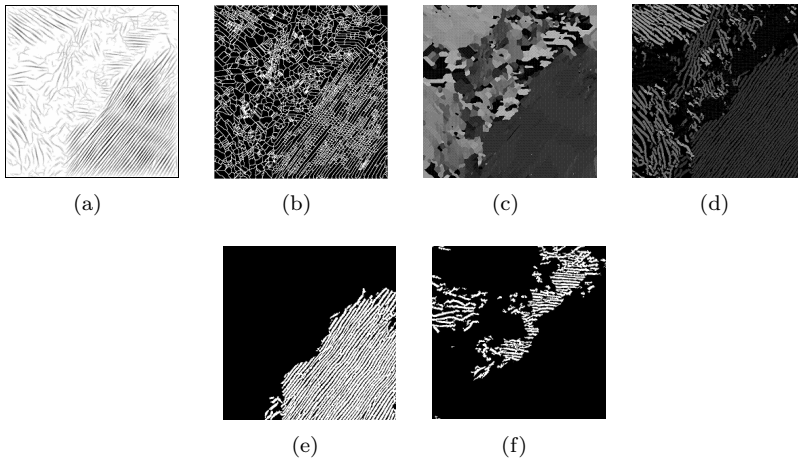Figure 5(a) shows the inverse image of image Dm in Figure 4(c), while

Figure 5. (a) Inverse line-segment function. (b) Watershed image. (c) Weigthed
catchment basins. (d) Segmented image. (e, f) Connected components.

Figure 5(b) illustrates its watershed image. To realize the merging process
it is preferable to work with the catchment basins associated with the water-
shed image. Figure 5(c) shows the catchment basins weighted by the values
of the angles of the regional maxima of the image Om of Figure 4(d). Now,
by analyzing a region of the image of Figure 5(c), one can identify the neigh-
boring regions with more-or-less similar orientations. In order to take into
account their neighborhood relationships, a region adjacency graph (RAG)
must be computed. In fact, the RAG simplifies the merging process. We
have chosen the method proposed in [13] for the merging process. Let us
introduce some concepts concerning graphs.

A graph is a pair made of a set V of vertices and a family of arcs.

Here, one considers the case of a graph without loops. This means that
there are no arcs connecting a vertex to itself. In the general case, arcs are
oriented; in this work, however, one takes the case of non-oriented graphs:
if there exists an arc joining vertex v to vertex v', then there also exists an
arc joining v' to v.

A vertex v' is said to be a neighbor of a given vertex v if there exists an
arc joining v to v'.

Thus, one way to represent a RAG consists of associating a vertex to
each region and an edge to each pair of adjacent regions. By definition the
RAG provides a *simple connectivity view* of the image. Beyond this simple
connectivity view this graph also gives a *high-level connectivity view* of the
image. Consider three regions A, B and C of an image. Thus, if two regions
A and B are adjacent, and also the regions B and C are adjacent, but A
and C are not adjacent, that leads us to consider that regions A and C have
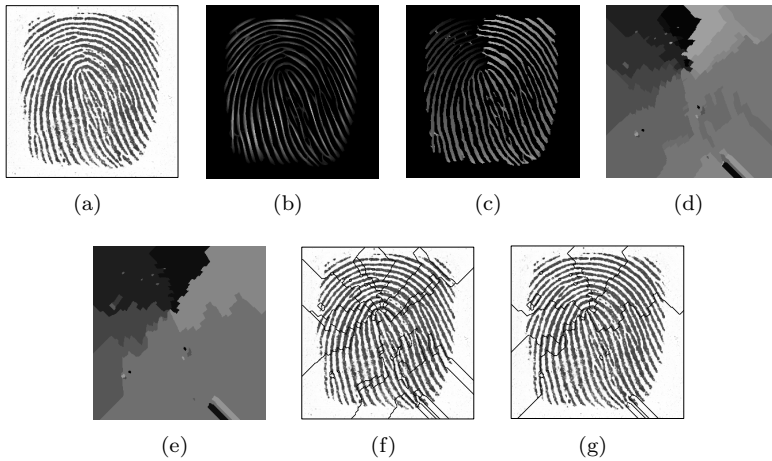a second order connectivity relationships.

Figure 6. (a) Original image. (b, c) Line-segment and orientation functions. (d, e) Images computed after the merging process using criteria values of 10 and 20 degrees, repectively. (f, g) Contours imposed to the original image.

In fact, the simple connectivity view contains inherently all *high-level connectivity relationships* of the image. Each vertex v_i corresponds a region R_i with orientation values (for example, $\overrightarrow{\mu}_i$ and $\overrightarrow{\sigma}_i$ mean value and variance value of the region) representative of the orientation distribution of this region. Each edge e_{ij} represents a pair of adjacent regions $\{R_i, R_j\}$ with a corresponding orientation distance $d(R_i, R_j)$, which can be used to compare the orientation distribution of these two regions. In our case, the computation of the RAG, using the angles of the regions, guides the subsequent merging of regions and provides a complete description of the neighborhoods. The RAG graph is constructed by use of the catchment basins of the image of Figure 5(c).

One takes a point from each minimum of the inverse line-segment function for representing each catchment basin. Remember that the inverse distance function is used. Since the graph under study is a valued, one must introduce some numerical values. Each edge is then assigned a value given by the absolute value of the difference between the angles of two neighboring regions, computed from the orientations image. The neighborhood graph of the maxima of the line-segment function and the directional function synthesize the directional field of the image. Two vertices of the graph are linked by an edge if the catchment basins are neighbors, and the value of the edge represents the directional similarity. One the regions are codified on a graph, we can compute the orientation fields based on the valued graph.

The following method (see [13]) for reducing the numbers of regions was carried out.

1. Each border has assigned an angle distance between the two regions it separates.

2. The borders are sorted in increasing order.

3. Two regions separated by the least value border are merged.

4. Step 2 is repeated until the criterion cannot be satisfied.

We illustrate the method by identifying the adjacent regions with more-or-less similar orientation by considering the image of Figure 4(a), a micrograph of the pearlite structure in steel. To achieve such a goal, one merges the vertices (catchment basins) with a difference of angles smaller than or equal to a given angle value $d(R_i, R_j) = |angle(R_i) - angle(R_j)| \leq \theta$. Figure 5(d), shows the segmented image of the orientation function of Figure 5(c), while Figures 5(e) and 5(f) show some connected components after the merging process using angles difference criterion θ of 20. The same approach was carried out with the fingerprint image shown in Figure 6(a). Figures 6(b) and 6(c) illustrate the line-segment function and the orientation function, whereas in Figures 6(d) and 6(e), one shows the images computed after the merging process using criteria values θ of 10 and 20, respectively. Finally, Figures 6(f) and 6(g), illustrate the contours imposed to the original image.

7. Conclusion and future works

This paper has shown the possibilities for application of morphological directional transformations to segment images with orientation fields. Initially, one investigates the directional granulometries and the notion of quadtree structure. The quadtree is used to describe a class of hierarchical data structures; thus it permits one to classify the orientation fields at different scales. After some drawbacks of this approach are illustrated, one considers a second local approach. This approach involves a local analysis using the notions of the line-segment and orientation functions proposed in this paper. The maxima of the line-segment function were used for computing the loci of maximal structuring elements, and the orientation function was used to obtain the angles of the line segments. These pairs of local parameters enable us to produce a good description of the image by means of line segments. Then, a partition of the image may be computed by means of the catchment basins associated with the watershed transform. This enables us to realize a neighborhood analysis, using a RAG structure, in order to merge adjacent regions of the partition according to appropriate criteria, thus segmenting the images into orientation fields. The results based on the algorithms presented in this paper show the good performance of the approach. Future work will be in the direction of seeking for an optimal segmentation based on lattice approach for morphological image segmentation proposed recently by Serra [11].

Acknowledgements

References

[1] C. Bahlmann, *Directional features in online handwriting recognition*, Pattern Recognition **39** (2006), 115–125.

[2] R. Cappelli and A. Lumini, *Fingerprint classification by directional image partitioning*, IEEE Trans. on Pattern Anal. Machine Intell **21** (1999), no. 5, 402–421.

[3] J. Crespo, R. Schafer, J. Serra, C. Meyer, and C. Gratin, *A flat zone approach: A general low-level region merging segmentation method*, Signal Proces. **62** (1997), 37–60.

[4] H. J. A. M. Heijmans, *Morphological image operators*, Academic, Boston, 1994.

[5] D. Jeulin and M. Kurdy, *Directional mathematical morphology for oriented image restoration and segmentation*, Acta Stereologica **11** (2001), 545–550.

[6] J. K. Lee, T. S. Newman, and Gary G. A., *Oriented connectivity-based method for segmenting solar loops*, Pattern Recognition **39** (2006), 246–259.

[7] J. Li, W. Y. Yau, and Wang H., *Constrained nonlinear models of fingerprint orientations with prediction*, Pattern Recognition **39** (2006), 102–114.

[8] J. Meyer and S. Beucher, *Morphological segmentation*, J. Vis. Comm. Image Represent. **1** (1990), 21–46.

[9] C. H. Park, J. J. Lee, M. J. T. Smith, and K. H. Park, *Singular point detection by shape analysis of directional fields in fingerprints*, Pattern Recognition **39** (2006), 839–855.

[10] J. Serra, *Image analysis and mathematical morphology*, Academic, London, 1982.

[11] _____, *A lattice approach to image segmentation*, J. Mathematical Imaging and Vision **24** (2006), no. 1, 83–130.

[12] _____, *Image analysis and mathematical morphology*, Academic, London, 1988.

[13] L. Shafarenko, M. Petrou, and Kittler J., *Automatic watershed segmentation of randomly textured color images*, IEEE Trans. on Image Processing **6** (1997), no. 11, 1530–1544.

[14] P. Soille, E. J. Breen, and R. Jones, *Recursive implementation of erosions and dilations along discrete lines at arbitrary angles*, IEEE Trans. on Pattern Anal. Machine Intell **18** (1996), no. 5, 562–567.

[15] P. Soille and H. Talbot, *Directional morphological filtering*, Pattern Recognition **23** (2001), no. 11, 1313–1329.

[16] A. Tuzikov, P. Soille, D. Jeulin, and P. Vermeulen, *Extraction of grid patterns on stamped metal sheets using mathematical morphology*, International Conference on Pattern Recognition, 1 (1992), pp. 425–428.